A Comparison Study of Advanced State Observer Design Techniques

Weiwen Wang and Zhiqiang Gao
The Applied Control Research Laboratory
Department of Electrical and Computer Engineering
Cleveland State University, Cleveland OH 44114

ABSTRACT

This paper presents a comparison study of performances and characteristics of three advanced state observers, including the high-gain observers, the sliding-mode observers and the extended state observers. These observers were originally proposed to address the dependence of the classical observers, such as the Kalman Filter and the Luenberger Observer, on the accurate mathematical representation of the plant. The results show that, over all, the extended state observer is much superior in dealing with dynamic uncertainties, disturbances and sensor noise. Several novel nonlinear gain functions are proposed to address the difficulty in dealing with unknown initial conditions. Simulation and experimental results are provided.

I. INTRODUCTION

Since the original work by Luenberger [1], the use of state observers proves to be useful in not only system monitoring and regulation but also detecting as well as identifying failures in dynamical systems. Since almost all observer designs are based on the mathematical model of the plant, the presence of disturbances, dynamic uncertainties, and nonlinearities pose great challenges in practical applications. Toward this end, the high-performance robust observer design problem has been topic of considerable interest recently, and several advanced observer designs have been proposed. A high-gain observer was first introduced by Khalil and Esfandiari [2] for the design of output feedback controllers due to its ability to robustly estimate the unmeasured states while asymptotically attenuating disturbances. Since then it has been used in solving many nonlinear system problems. For example, H. Rehbinder, X. Hu et al. [3] used it to estimate nonlinear pitch and roll for walking robots. K.W.Lee et al. [4] designed a robust output feedback control of robot manipulators with it. Another proposed observer design is based on the sliding-mode principle. The sliding–mode design method enhances robustness over a range of system uncertainties and disturbances. The earlier work was introduced by Slotine [5] and Utkin [6]. R. Sreedhar, B.Fernandez and G.Y.Masada [7] used it for robust fault detection in nonlinear systems. F.J.J.Hermans and M.B.Zarrop [8] presented robust sensor monitoring using sliding-mode observers. A class of nonlinear extended state observers (NESO) was proposed by J. Han [9] in 1995 as a unique observer design. It is rather independent of mathematical model of the plants, thus achieving inherent robustness. It was tested and verified in key industrial control problems [10, 11].

This paper presents a comparison of performances and characteristics of these observers. The criterion for comparison is based on the observer tracking errors, both at steady state and during transients, and the robustness of the performance with respect to the uncertainties of plant. To further enhance the performance of NESO in the presence of unknown initial conditions, several nonlinear gain functions are introduced. The simulations conducted assisted in gaining insight of observer behavior in both open-loop and closed–loop scenarios. The experimental results are also provided to give realism.

The organization of the paper is as follows. Section II gives an introduction to existing observer design techniques. In Section III, simulation results of three observers in both open-loop and closed-loop forms are presented. A comparison of several nonlinear gains for NESO is also performed. The experimental results are presented in Section IV and concluding remarks are given in Section V.

II. THE EXISTING OBSERVERS

Consider a linear, time-invariant, continuous-time dynamic system

$$\begin{aligned} \dot{x} &= Ax + Bu \\ y &= Cx \end{aligned} \tag{1}$$

where the matrices A, B and C are parameters of the state space model. The well-known Luenburger Observer is given as

$$\dot{\hat{x}} = A\hat{x} + Bu + L(y - C\hat{x}) \tag{2}$$

The estimation error is

$$e = x - \hat{x} \tag{3}$$

The error dynamic equation is

$$\dot{e} = (A - LC)e = \hat{A}e \tag{4}$$

The estimation error will converge to zero if $\hat{A} = A - LC$ has all its eigenvalues in the left-half plane. The observer design refers to the selection of the gain matrix L, using, for example, the pole placement method.

The observer is a very useful tool for receiving the information of the internal variables of a system that are otherwise unknown. For this reason, it is used widely in control, estimation, and other engineering applications. The main challenge in these applications is that the observer design is heavily dependent on the accuracy of the mathematical model of the plant, in this case, the A, B, and C matrices. To enhance the capabilities of observers in dealing with real world issues, such as uncertainty, noise, disturbance, etc., several advanced techniques were proposed and are briefly introduced below. More detailed descriptions can be found in the corresponding references.

For the sake of simplicity and comparison, a second order nonlinear system is considered, described by

$$\ddot{y} = f(y, \dot{y}, w) + b_0 u \tag{5}$$

where $f(.)$ represents the dynamics of the plant and the disturbance, w is the unknown input disturbance, u is the control signal, and y is the measured output. The parameter b_0 is assumed to be given. Note that $f(.)$ is usually a nonlinear function.

2.1 High-gain Observers

The high-gain observer (HGO) [12] for the plant (5) is designed as:

$$\begin{aligned}\dot{\hat{x}}_1 &= \hat{x}_2 + h_1(y-\hat{x}_1)\\ \dot{\hat{x}}_2 &= f_0(.) + b_0 u + h_2(y-\hat{x}_1)\end{aligned} \tag{6}$$

where $f_0(.)$ is a nominal model of the nonlinear function $f(.)$. The estimation error equations are

$$\begin{aligned}\dot{\tilde{x}}_1 &= -h_1\tilde{x}_1 + \tilde{x}_2\\ \dot{\tilde{x}}_2 &= -h_2\tilde{x}_1 + \delta(x,\tilde{x})\end{aligned} \qquad \tilde{x} = \begin{bmatrix} x_1 - \hat{x}_1 \\ x_2 - \hat{x}_2 \end{bmatrix}$$

where $\delta(.) = f(.) - f_0(.)$. In the absence of the disturbance term $\delta(x,\tilde{x})$, asymptotic error convergence is achieved by designing the observer gain such that the matrix

$$A_0 = \begin{bmatrix} -h_1 & 1 \\ -h_2 & 0 \end{bmatrix}$$

is Hurwitz. For this second-order system, A_0 is Hurwitz for any positive constants h_1 and h_2. In the presence of δ, the observer gains are adjusted as

$$h_1 = \frac{\gamma_1}{\varepsilon}, h_2 = \frac{\gamma_2}{\varepsilon^2} \tag{7}$$

where $0 < \varepsilon << 1$, and the gain γ_1, γ_2 can be determined via pole placement. Adjustments were made in (7) is to make the transfer function from δ to $\tilde{x}$ small so that the estimation error is not sensitive to the modeling error.

2.2 The Sliding-mode Observers

The sliding-mode observer (SMO) for the nonlinear system (5) is defined by [5]

$$\begin{aligned}\dot{\hat{x}}_1 &= \gamma_1(y-\hat{x}_1) + \hat{x}_2 + k_1 sign(y-\hat{x}_1)\\ \dot{\hat{x}}_2 &= \gamma_2(y-\hat{x}_1) + f_0 + b_0 u + k_2 sign(y-\hat{x}_1)\end{aligned} \tag{8}$$

The constants γ_1 and γ_2 are selected to place the poles of the linearized system at desired locations. The switching gain k_1 is a bound on the steady state estimation error on x_2, and k_2 is chosen to be larger than the modeling error $\delta(.)$.

2.3 Nonlinear Extended State Observers

The previous two methods, much like most classical state observer designs, depend on the knowledge of the plant dynamics, $f(y,\dot{y},w)$. An alternative method is given by Han [9] as follows. The plant in (5) is first augmented as

$$\begin{cases}\dot{x}_1 = x_2\\ \dot{x}_2 = x_3 + b_0 u\\ \dot{x}_3 = h\\ y = x_1\end{cases} \tag{9}$$

where $f(y,\dot{y},w)$ is treated as an extended state, x_3. Here both $f(y,\dot{y},w)$ and its derivative $h = \dot{f}(y,\dot{y},w)$ are assumed unknown. By making $f(y,\dot{y},w)$ a state, however, it is now possible to estimate $f(y,\dot{y},w)$ by using a state estimator. Han proposed a nonlinear observer for (9) as [9]:

$$\begin{cases}\dot{z}_1 = z_2 + \beta_1 g_1(e)\\ \dot{z}_2 = z_3 + \beta_2 g_2(e) + b_0 u\\ \dot{z}_3 = \beta_3 g_3(e)\end{cases} \tag{10}$$

where $e=y-z_1$. z_3 is the estimate of the uncertain function $f(.)$. $g_i(.)$ is defined as a modified exponential gain function:

$$g_i(e,\alpha_i,\delta) = \begin{cases} |e|^{\alpha_i} sign(e), |e| > \delta \\ \dfrac{e}{\delta^{1-\alpha_i}}, |e| \le \delta \end{cases} \quad \delta > 0, \tag{11}$$

This observer is denoted as the nonlinear extended state observer (NESO). As α_i is chosen between 0 and 1, g_i yields high gain when error is small. δ is a small number used to limit the gain in the neighborhood of origin. Starting with linear gain $g_i(e,\alpha_i,\delta) = e$, the pole placement method can be used for the initial design of this observer, before the nonlinearities are added to enhance the performance. A detailed design and tuning method for the linear extended state observer (LESO) is demonstrated in [17].

2.4 Selection of Nonlinear Gains for NESO

Research revealed that, for the plant with unknown initial conditions, a new nonlinear function $f_i(.)$, as shown in equation (12), can be used in NESO to avoid significant transient estimation error:

$$f_i(e,k_{1i},k_{2i}) = \begin{cases} k_{2i}e + sign(e)*(k_{1i}-k_{2i})*\delta, |e| > \delta \\ k_{1i}*e, |e| \le \delta, \delta > 0 \end{cases} \tag{12}$$

with $k_{1i}, k_{2i} > 0$. Furthermore, by choosing $\alpha_i < 0$ in (11), the transient error is significantly reduced. Three curves from (11) and (12) are shown in Figure 1 to illustrate the differences. As in (11), δ defines the range of a high gain section where the observer is very aggressive. This range is usually small.

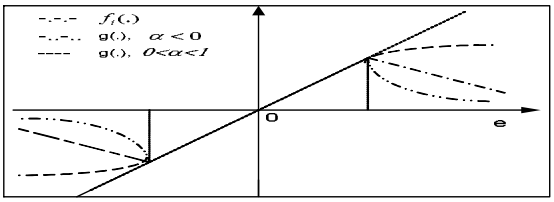

Figure 1: Nonlinear gain functions

III. COMPARISON IN SIMULATION

An industrial motion control test bed made by ECP [13] is used for simulation. Its linear model was derived as:

$$\ddot{y} = -1.41\dot{y} + 23.2u \tag{13}$$

where y is the output position and u is the control voltage sent to the power amplifier that drives the motor. Selecting the observer poles at –4.2, $\{\gamma_1, \gamma_2\}$ in HGO and SMO, and $\{\beta_i, i = 1,2,3\}$ in NESO are determined via pole-placement. In addition, ε=. 2 is used for the HGO, k_1=. 5 and k_2=15 are used for the SMO, and $\alpha_i = \{1, .5, .25\}$ and δ=10^{-3} are used for the NESO. All three observers were implemented digitally with a sampling rate of 1 kHz. The output measurement is corrupted by white noise to make the comparison realistic. The quality of observers is measured by the speed and accuracy of the states of the observer converging to those of the plant. To make the comparison fair, the parameters of the observers are adjusted so that their sensitivities to the measurement noise are roughly the same. The exact outputs of y and $\dot{y}$ are obtained directly from the

simulation model of the plant to calculate the state estimation error.

During simulation, open-loop tests were performed, followed by closed-loop tests.

3.1 Open-loop Comparison

In the case of open-loop tests, the input to the plant is a step function and the observers are evaluated according to their capability in tracking the step response. The tests were run in three conditions:

- Nominal plant;
- Nominal plant plus coulomb friction;
- Nominal plant with 100% increase in inertia.

The same set of observer parameters are used in all simulations. Figure 2 shows the position and velocity estimation errors for the nominal plant in terms of the tracking errors for y and $\dot{y}$. For all three observers perform well in steady state and have roughly the same accuracy and sensitivity to the noise. As expected, NESO takes longer to reach steady state, as expected, because it does not assume the knowledge of the plant dynamics. Interestingly, z_3 converges to the unknown function $f = -1.41\,\dot{y}$, as shown in Figure 3.

Figure 4 illustrates the tracking errors for plant with added coulomb friction, clearly demonstrating that NESO is much more robust than HGO and SMO in the presence of disturbance. Once again, z_3 converges quickly and accurately to the combination of unknown dynamics and disturbance, $a(t) = f(y, \dot{y}, w)$, as shown in Figure 5.

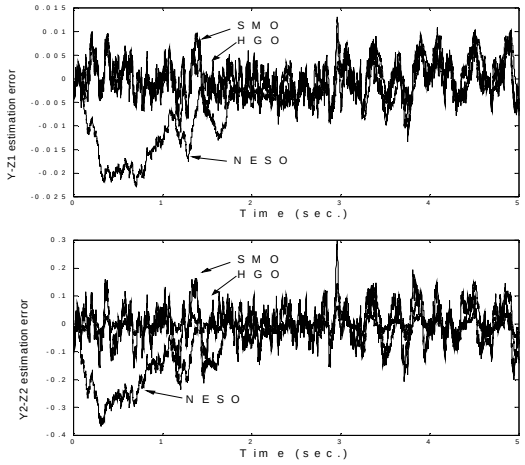

Figure 2: Estimation error of the nominal plant

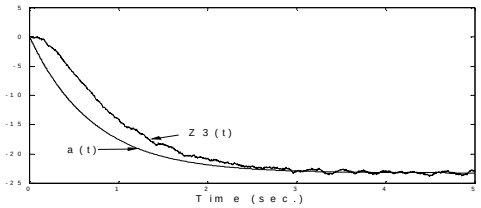

Figure 3: $x_3 = a(t)$ and its estimation z_3

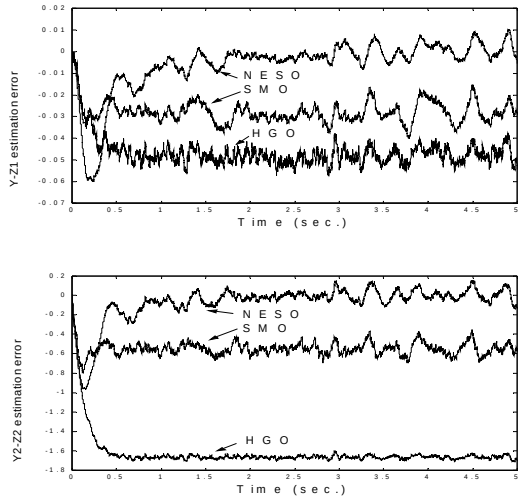

Figure 4: Estimation error of the plant with 0.5N-m coulomb friction

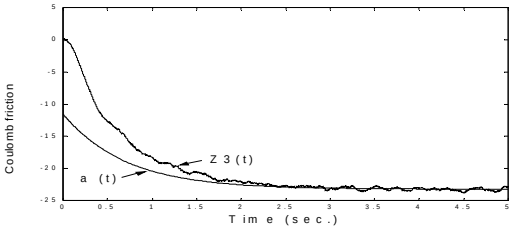

Figure 5: Disturbance and its estimation

Figure 6 and 7 illustrate the simulation results for the plant with a 100% increase of inertia. Once again NESO provides an overall superior performance, followed by SMO.

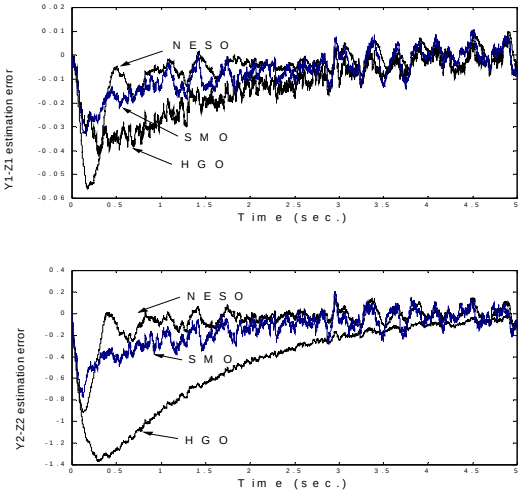

Figure 6: Estimated error with 100% change of inertia

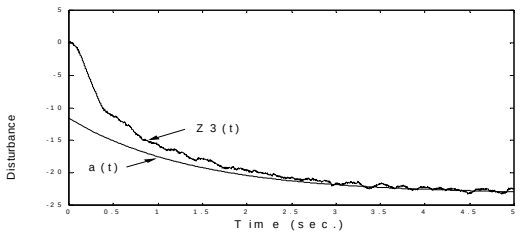

Figure 7: Disturbance and its estimation

3.2 Effects of NESO Gains Adjustment with Unknown Initial Conditions

Simulations reveal that NESO achieves better performance among these observers. However, if the plant has unknown initial conditions, it may produce significant transient estimation errors. The following simulation tests were performed for the comparisons of three gain functions for NESO as shown in Figure 1. The initial conditions are set as $y(0) = 10$ (rev) and $\dot{y}(0) = 0$. The observer poles used in simulation are placed at –8 rad/sec. The simulation results are shown in Figure 8.

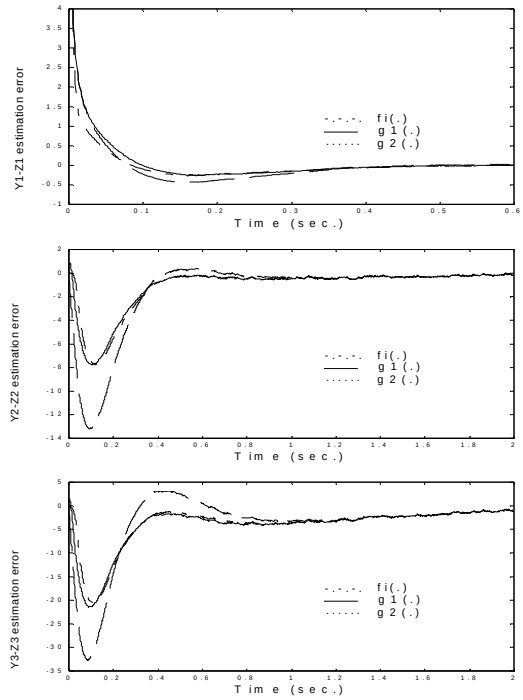

Figure 8: Estimated error of the plant with initial values

The corresponding gain parameters used in simulation are:

$f_i(.)$: $k_{11} = 24, k_{12} = 192, k_{13} = 512,\ \delta_1 = \delta_2 = \delta_3 = 1,$
$k_{21} = 200, k_{22} = -60, k_{23} = -130.$

$g_1(.)$: $k_{11} = 24, k_{12} = 192, k_{13} = 512,\ \delta_1 = \delta_2 = \delta_3 = 1$
$\alpha_1 = 2, \alpha_2 = -4, \alpha_3 = -4.$

$g_2(.)$: $k_{11} = 24, k_{12} = 192, k_{13} = 512,\ \delta_1 = \delta_2 = \delta_3 = 1,$
$\alpha_1 = 2, \alpha_2 = .2, \alpha_3 = .2.$

The simulation results indicate clearly that the $f_i(.)$ and the $g_1(.)$ functions achieve better performance with smaller tracking errors. The results also suggest that the negative power should be used in (11) to counter unknown initial conditions.

3.3 Closed-loop Comparison

Based on their open loop performance, NESO and SMO are evaluated in a closed-loop feedback setting, such as that shown in Figure 9 for NESO. The profile generator provides the desired state trajectory in both y and $\dot{y}$, using an industry standard trapezoidal profile. Based on the separation principle, the controller is designed independently, assuming that all states are accessible in the control law.

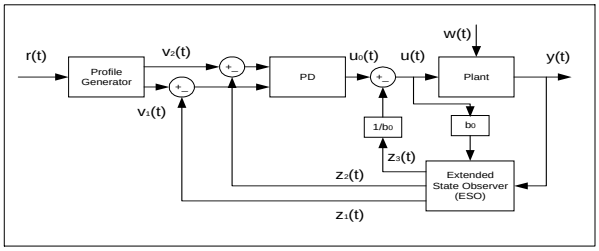

Figure 9: Observer Based State Feedback Control Configuration

In the case of NESO, the extended state information, z_3, which converges to $x_3 = f(y, \dot{y}, w)$, is used to compensate for the unknown $f(y, \dot{y}, w)$. In particular, the control law is given as

$$u = (-z_3 + Ke)/b_0 \tag{14}$$

where $e = [v_1 - z_1 \ \ v_2 - z_2]^T$ and K is the state feedback gain that is equivalent to a proportional-derivative (PD) controller design. Substituting (14) in (5),

$$\ddot{y} = (f(y, \dot{y}, w) - z_3) + Ke \tag{15}$$

K can be determined via pole-placement. More details about this design strategy can be found in [10, 11, 14-17].

For SMO-based state feedback design, only the position and velocity estimates, z_1 and z_2 are available and the corresponding PD design yields the following closed-loop system,

$$\ddot{y} = f_0(y, \dot{y}, w) + Ke = -1.41\,\dot{y} + Ke \tag{16}$$

Note that the extended state, z_3, is not available in SMO. The poles of observers are selected as –12 rad/sec. For the controller design, the closed-loop poles are placed at –15 rad/sec. In addition, $k_1 = .5$ and $k_2 = 15$ are used for the SMO, and $\alpha_i = \{1, .5, .25\}$ and $\delta = 10^{-3}$ are used for the NESO. For the sake of fairness, the same observer and control poles are used for both NESO and SMO based designs. The main difference in design is that the NESO based method assumes no knowledge of $f(y, \dot{y}, w)$.

Simulation results are shown in Figure 10, 11, and 12. Both control systems have similar output responses for the nominal plant. However, as soon as unknown friction or disturbances are introduced, the differences between NESO and SMO become apparent, indicating that the NESO-based design has inherent robustness against the uncertainties. By estimating $f(y, \dot{y}, w)$, instead of modeling it, the controller becomes independent of it.

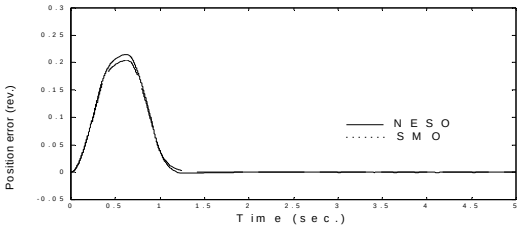

Figure 10: Nominal responses of the control systems

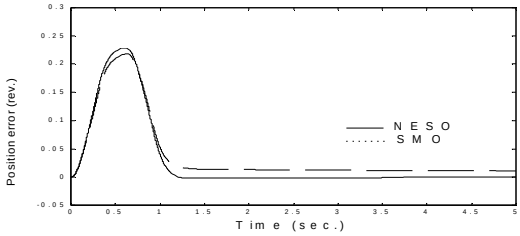

Figure 11: Simulation results with 0.5 N-m coulomb frictions

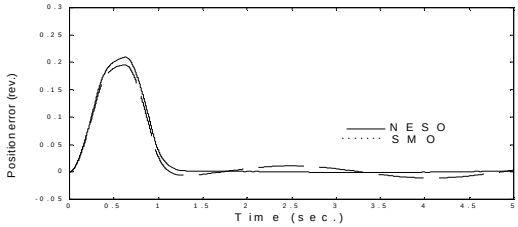

Figure12: Simulation results with sinusoid disturbance

IV. HARDWARE TEST RESULTS

An industrial motion control test bed is used to verify the above results and show potential practical applications. The setup includes a PC based control platform and a DC brushless servo system, shown in Figure 13. The servo system includes two motors, one as an actuator, and the other as a disturbance source; a power amplifier and an encoder that provides the position measurement. The inertia, friction and backlash are all adjustable, making it convenient to test the control algorithms. A Pentium 133 MHz PC running in DOS is programmed as the controller. It contains a data acquisition board for digital to analog conversion and a counter board to read the position encoder output signal. The sampling frequency is 1 kHz. The output of the controller is limited to $\pm$ 3.5 V. The drive system has a dead zone of $\pm$ 0.5 V.

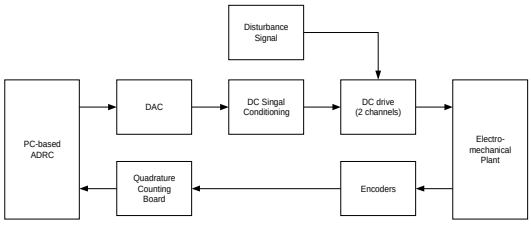

Figure 13: A diagram for DC brushless servo system

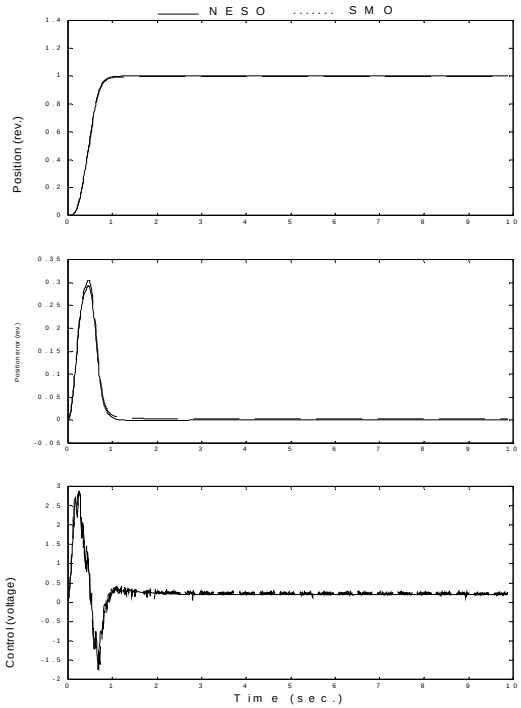

Figure 14: Responses to the nominal plant

The plant is modeled using approximation as it was in (13). Initially no friction, disturbance or backlash is intentionally added. To verify the effectiveness of the NESO, the same control poles are used for both the NESO-based and SMO-based control systems. The response of the nominal system is plotted in Figure 14. Figure 15 shows the response of the plant having coulomb friction. The results indicate that NESO-based controller performs better in both steady state accuracy and the transient response. A chattering problem is also apparent in the SMO-based design.

In general, the hardware test results are consistent with those of the software simulations.

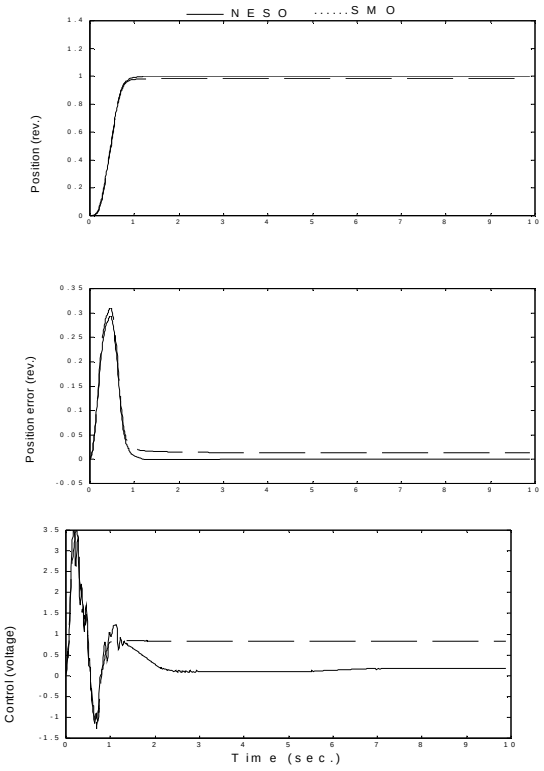

Figure15: Responses to coulomb friction

V. Concluding Remarks

A comparison study of advanced observer designs, including the nonlinear extended state observer, the high-gain observer, and the sliding-mode observer, was performed. A gain modification method is proposed for the nonlinear extended state observer to deal with the unknown initial conditions. Both software simulation and hardware tests are performed. The following observations are made based on the results:

- As a state estimator, NESO performs better than the high-gain observer and the sliding-mode observer. The robustness of the NESO to plant uncertainty and external disturbance is inherent in its structure. The chattering problem is the main drawback of the sliding-mode method in practical applications.

- The simulation and experimental results seem to justify the design concepts of NESO. Specifically, by augmenting the plant and making the unknown dynamics as an extended state, an alternative design method for state observers and an alternative to system identification were discovered. That is, instead of trying to find a mathematical expression of the dynamics and disturbances, a state observer can be built to estimate it and compensate for it in real time.

REFERENCES

[1] D. Luenberger, "Observers for multivariable systems", IEEE Trans. Autom. Control, 11, 190-197, 1966.

[2] F. Esfandiari and H.K. Khalil. "Output feedback stabilization of fully linearizable systems", Int. J.Control, 56:1007-1037, 1992.

[3] H. Rehbinder and X. Hu. "Nonlinear pitch and roll estimation for walking robots", Proceedings of the 36th Conference on Decision & Control, San Diego, CA USA. December 1997, pp: 4348-4353.

[4] E.S. Shin, K.W. Lee. "Robust output feedback control of robot manipulators using high-gain observer", Proceedings of 1999 IEEE International Conference on Control Application. Hawaii, USA. August 22-27, 1999.

[5] J.J.E. Slotine, J.K .Hedrick, and E.A. Misawa, "On sliding observers for nonlinear systems", Journal of Dynamic Systems, Measurement, and Control. Vol.109, 1987, pp: 245-252.

[6] V.I. Utkin. *Sliding-modes in control optimization*. Springer-Verlag, 1992.

[7] R.Sreedhar, B.Fernandez and G.Y.Masada. "Robust fault detection in nonlinear systems using sliding-mode observers", Proceedings of IEEE Conference on Control Applications, September 13-16, 1993 Vancouver, BC.

[8] F.J.J. Hermans and M.B. Zarrop. "Sliding-mode observers for robust sensor monitoring", Proceedings of 13th IFAC World Congress, SanFrancisco, USA, 1996, pp: 211-216.

[9] J. Han. "A class of extended state observers for uncertain systems", Control and Decision, Vol.10, No.1, pp: 85-88, 1995. (In Chinese)

[10] Y. Hou, Z. Gao, F. Jiang and B.T. Boulter. "Active disturbance rejection control for web tension regulation", Proceedings of the 40th IEEE Conference on Decision and Control, Orlando, Florida USA, December 2001, pp: 4974-4979.

[11] Z. Gao, S. Hu and F. Jiang. "A novel motion control design approach based on active disturbance rejection", Proceedings of the 40th IEEE Conference on Decision and Control, Orlando, Florida USA, December 2001, pp: 4877-4882.

[12] Khalil, H.K. "High-gain observers in nonlinear feedback control. New Directions in Nonlinear Observer Design" (Lecture Notes in Control and Information Sciences) Vol. 24(4). 1999. pp: 249-68.

[13] Manual for Model 220 Industrial Emulator/Servo Trainer, Educational Control Products, 5725 Ostin Avenue, Woodland Hills, CA 91367, 1995.

[14] J. Han, "Nonlinear Design Methods for Control Systems", The Proc. Of The 14th IFAC World Congress, Beijing, 1999.

[15] Z. Gao, "From Linear to Nonlinear Control Means: a Practical Progression," Presented at the ISA Emerging Technology Conference, September 12, 2001; ISA Transactions, vol.41, no.2 p. 177-89, April 2002.

[16] Z. Gao, Y. Huang and J. Han, "An Alternative Paradigm for Control System Design," Proc. Of the 40th IEEE Conference on Decision and Control, Orlando, Florida USA, December 2001, pp: 4578-4585.

[17] Z. Gao, "Scaling and bandwidth-parameterization based controller-tuning", to be presented at the 2003 American Control Conference, Denver, Colorado, June 2003.